

*Scientific Paper*Doi: <http://dx.doi.org/10.1590/1809-4430-Eng.Agric.v44e20230131/2024>**DESIGN AND OPTIMIZATION TEST OF HIGH-SPEED SEED GUIDE DEVICE WITH CONICAL SPIRAL AIRFLOW****Sihao Zhang¹, Huaijiang Zhu¹, Wenjun Wang^{1*}, Yulong Chen¹,
Long Zhou¹, Mingwei Li¹, Jida Wu^{1,2}**¹*Corresponding author. School of Agricultural Engineering and Food Science, Shandong University of Technology/Zibo, China.E-mail: wjwang2016@163.com | ORCID ID: <https://orcid.org/0000-0001-7101-3763>**KEYWORDS**

high-speed, conical spiral airflow, multifactor central composite test, precision seeding, seed guide technology and device.

ABSTRACT

During high-speed seeding operations, collisions between seeds and seed guide tubes are very significant, resulting in poor seed spacing uniformity. To solve this problem, a high-speed seed guide device with conical spiral airflow was designed, which can use high-speed positive pressure airflow to move seeds smoothly. To improve the uniformity of the airflow field in the device, a single-factor test was carried out to determine the reasonable range of each factor. Then, the four-factor and five-level central composite test was carried out. The four main factors were screw pitch, cone angle, width of gap, and angle of air-tube, and the evaluation index was the mean variance of airflow velocity. The test results showed that the optimal parameters of the high-speed seed guide device with conical spiral airflow were a screw pitch of 24.98 mm, cone angle of 7.47/55, width of gap of 5.31 mm, and angle of air-tube of 25.09°. The verification test showed that the relative error between the verification test value and the predicted value was less than 5%, indicating that the model had high reliability. This research can provide references for the research of high-speed seed guide technology and the innovative design of seed guide devices.

INTRODUCTION

Seeding operation is one of the most important components in the large-scale field agricultural production process, which directly affects the germination of seeds and the emergence and growth of crops (Dhillon et al., 2022). Therefore, the high quality of mechanized seeding operations is an important basis for ensuring food security and promoting agricultural harvest under the condition of limited cultivated land resources. With the development of high efficiency, high quality, green and sustainability modern agriculture (Wang et al., 2022 a), agricultural producers have put forward higher requirements for the speed and accuracy of seeding operations (Ding et al., 2021), making high-speed precision seeding technology gradually becoming an important development direction and trend in field operations.

However, it is difficult to accurately control seed movement during high-speed operations, especially when the seeds are moving in the guide tube. When seeds leaving the seed-metering device enter the seed guide tube, due to the different incident angles, machine vibration and tilt, the seeds

will disorderly collide in the seed guide tube (Wang et al., 2022 b; Zhou et al., 2020). The random collisions will cause seeds to fail to move in accordance with the predetermined trajectory, resulting in changes in the relative position of seeds in the furrow and ultimately failing to meet the requirements of seeding operations (Yuan et al., 2018; Liu et al., 2022; Nardon & Botta, 2022; Yang et al., 2016). Therefore, research on seed guide technology and devices is of great significance for improving seeding quality.

To solve the problem of poor seeding quality caused by random seed collisions in seed guide tubes, scholars in the China and abroad have carried out in-depth research on seed guide technology and devices. According to the constraint types of seeds, seed guide devices are mainly divided into two categories: seed guide devices with passive constraints and seed guide devices with active constraints (Liao et al., 2020).

The seed guide device with passive constraint is a seed guide tube, in which the seeds move under their own gravity. Reasonable structural design of the seed tube can realize effective constraints on the seed moving path. Therefore,

¹ School of Agricultural Engineering and Food Science, Shandong University of Technology/Zibo, China.² School of Mechanical and Electrical Engineering, China University of Mining and Technology/Xuzhou, China.

Area Editor: Tiago Rodrigo Francetto

Received in: 9-24-2023

Accepted in: 11-13-2023



research has focused on the seed guiding curve and cross-section structure of seed guide tubes to obtain the optimal seed moving path (Kumar & Raheman, 2018; Yang et al., 2022; Carpes et al., 2017). (Chen et al., 2022) designed a combined seed tube composed of a joint section and a delivery section. By controlling the angles of the two sections, optimal seed guide curves at different speeds are formed, and the test results showed that the qualified rate of seed spacing of the combined seed tube was 15.1% higher than that of the traditional seed tube. (Liao & Shu, 2004) reported the effects of diameter, length and inclination of the seed guide tube on seed spacing uniformity, and the test results showed that the optimal combination of seed guide tubes was a diameter of 22 mm, a length of 500 mm and an inclination of 60°. (Wang et al., 2017) studied the steady migratory mechanism of a guiding-seed system to improve the guiding migration performance of a pickup finger precision seed metering device and analysed the influences of various factors on dropping trajectory and migration stability. (Liu et al., 2016) used the discrete element method to analyse the conveying process of maize seeds in seed guide tubes and found that the optimal height of the seed guide tube was 500 mm. (Li et al., 2020) proposed a linear seeding method and determined the parameters of the seed guiding curve through theoretical analysis. The test results showed that the qualified rate of seed spacing was improved by 4.22% compared with the traditional seed tube.

With increasing operation speed, seed guide devices with passive constraints have been unable to meet the needs of high-speed operation, and the research focus has gradually turned to seed guide devices with active constraints (Gao et al., 2022). (Zhao et al., 2018) designed a V-groove dialing round-type guiding-seed device, and the overall structure and working principle of the guiding-seed device were illustrated and analysed. (Ma et al., 2023) analysed the mechanism of corn seeds receiving by a rotating clamp for a belt-type high-speed seed guiding device and proposed an improvement method of adding herringbone lines on the surface of the pick-up finger. The seed guide device with an active constraint can effectively restrain the seeds to maintain the order state during the conveying process by mechanical structure and airflow, ensuring seed spacing uniformity during seed movement. (Chen & Zhong, 2012) designed a belt-type seed guide device whose speed matched the rotational speed of the seed plate and the forward speed of the planter. The test results showed that the qualified rate of seed spacing was 98.5%. (Kang et al., 2015) optimized the original belt-type seed guide device through bench tests and improved its seeding quality. (Wang et al., 2020 a) designed a pneumatic wheat precision seed casting device. Through fluent simulation analysis to

determine the key component parameters, and the test-bad shows the device can achieve accurate and stable single seed sowing. Based on better parameter combination conditions of work, the coefficient of variation of the seeding velocity and average depth was 8.3% and 5.8%, respectively. (Wang et al., 2020 b) designed a seed pressing device for precision seeders based on airflow-assisted seed delivery. The results of the bench test showed that the qualified rate of seed spacing and variation coefficient of seed spacing were 95.68% and 10.32%, respectively. (Liu et al., 2023) designed an airflow-assisted seed guide device based on the Venturi principle. The test results showed that when the forward speed was 16 km/h, the qualified rate of seed spacing increased by 13.6%, and the variation coefficient of seed spacing decreased by 7.4%.

The seed guide device with machine constraints mainly adopts various mechanical structures with active restraints, such as partition-type, belt-type, finger wheel-type and brush wheel-type structures (Wei et al., 2022), which can effectively reduce collisions during the seed conveying process and have good moving uniformity. However, seed guide devices with machine constraints have complex mechanisms, large power consumption, serious wear and poor high-speed reliability. In addition, the seed guide device using the friction conveying principle would cause some mechanical damage to seeds. The seed guide device with airflow constraints mainly adopted the structural form of a Venturi tube (Gao et al., 2018), and the research focused on optimizing the structural parameters of the seed guide device and the working parameters of airflow. The seed guide device with airflow constraints had the advantages of little seed damage and high conveying speed, but the airflow field was easily disturbed at the intersection of the seed tube and airflow tube, resulting in poor seed conveying uniformity and stability at the seed-airflow contact moment.

To solve the problem of airflow constraints in seed guide devices, a high-speed seed guide device with conical spiral airflow was designed. The device formed a conical spiral airflow through a spiral accelerator to ensure seed conveying uniformity and stability at the seed-airflow contact moment. At the same time, the seeds were accelerated under the action of high-speed airflow, which reduced the collision between seeds and the tube wall to improve the seed spacing uniformity. In this study, the single-factor test was first carried out to investigate the effects of each factor on airflow uniformity and determine the reasonable range of values for each factor. Then, the multifactor central composite test was carried out to find optimal parameter combinations. This research can provide references for the research of high-speed seed guide technology and the innovative design of seed guide devices.

MATERIAL AND METHODS

Structure and working principle of the high-speed seed guide device with conical spiral airflow

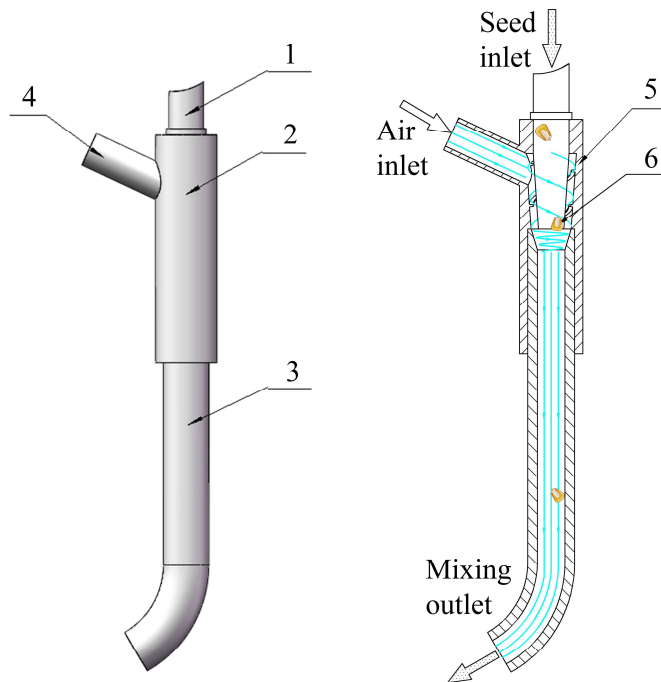


FIGURE 1. Schematic diagram of the feed type seed guide device.

1. Seed tube 2. Spiral accelerator 3. Mixed conveying tube 4. Air tube 5. Accelerator shell 6. Conical tube

The overall structure of the high-speed seed guide device with conical spiral airflow is shown in Figure 1, which mainly consisted of a seed tube, air tube, spiral accelerator and mixed conveying tube. The high-speed airflow can not only accelerate the falling seeds but also correct the moving path of seeds to realize the high-speed uniform transportation of seeds.

Working principle of the high-speed seed guide device with conical spiral airflow: The seeds leaving the seed-metering device drop into the seed tube and fall freely under the action of gravity. At the same time, the airflow generated by a blower enters the spiral accelerator through the air tube, forming a high-speed spiral airflow. When the seeds entered the spiral accelerator, the seeds were accelerated into the conveying tube under the action of the negative pressure airflow field generated by the spiral airflow, forming the high-speed gas-seed mixture flow. The high-speed seed guide device with conical spiral airflow can reduce the collision between seeds and the tube wall and finally enter the seed furrow to complete the entire seed conveying process.

Experimental conditions and methods

In this study, the software Solidworks 2019 was used to establish a three-dimensional model of the high-speed seed guide device with conical spiral airflow, and then the model was imported into the software Fluent 2020 R2 to simulate the airflow field. In the simulation analysis, the average variance of airflow velocity was used to measure the uniformity of the airflow field in the device, optimizing the structural parameters of the spiral accelerator.

Single-factor test

According to the above analysis of the structure and working principle of the high-speed seed guide device with

conical spiral airflow, the following five factors may have a greater impact on the uniformity of the airflow field: number of threads (NT), screw pitch (SP), cone angle (CA), width of gap (WG), and angle of air tube (AA) (Figure 2). To investigate the effects of each factor on the uniformity of the airflow field and to determine a reasonable range of values for each factor, a single-factor parameter optimization test was carried out.

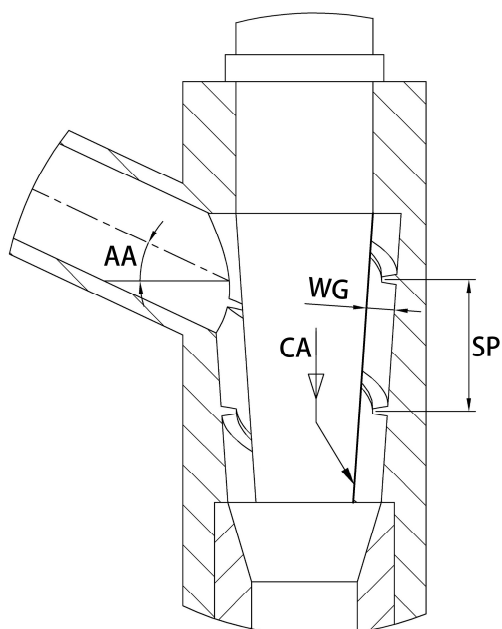


FIGURE 2. Structure of spiral accelerator.

SP: screw pitch; CA: cone angle; WG: width of gap; AA: angle of air tube

In the single-factor test, the initial airflow velocity was set to 7 m/s. Four parallel planes are selected as the measurement planes of the index, namely, the plane at the seed-airflow intersection and the planes 20 mm, 50 mm, and 170 mm away from it. The airflow velocity of each point was obtained by random and uniform sampling in the four planes, and the sample variance (V_{ar}) of each plane was calculated. Finally, the average value of the sample variances was taken as the test index. The equation is shown in eqs (1) and (2).

$$v_{ar} = \frac{1}{n-1} \sum_{i=1}^n (x_i - \bar{x})^2 \quad (1)$$

$$Y = \frac{1}{4} \sum_1^4 v_{ar} \quad (2)$$

in which:

v_{ar} -the sample variance of each plane;

n - the sample capacity;

x_i - the airflow velocity of the sample point;

\bar{x} - the mean airflow velocity.

Y - the average value of the sample variances

Multifactor central composite test

To study the interaction effects of several factors on the uniformity of the airflow field and determine the optimal parameter combination of the high-speed seed guide device with conical spiral airflow, a multifactor central composite

test was carried out.

In the single-factor test, a reasonable range of values for each factor was determined: screw pitch SP=20-25 mm, cone angle CA=6/55-8/55, width of gap WP=5-6 mm, and angle of air tube AA=25°-45°. The four-factor and five-level central composite test was carried out. The four factors were screw pitch (X_1), cone angle (X_2), width of gap (X_3) and angle of air tube (X_4). The evaluation method of the multifactor central composite test was the same as that of the single-factor test. The experimental factors and levels are shown in Table 1, and the design scheme is shown in Table 7.

TABLE 1. Test factors and levels.

Code	Factor			
	X_1/mm	X_2	X_3/mm	$X_4/^\circ$
-2	17.5	6/55	4.5	25
-1	20	6.5/55	5	30
0	22.5	7/55	5.5	35
1	25	7.5/55	6	40
2	27.5	8/55	6.5	45

RESULTS AND DISCUSSION

Results and analyses of the single-factor test

The single-factor test was carried out with the number of threads (NT), screw pitch (SP), cone angle (CA), width of gap (WG) and angle of air-tube (AA) as the test factors. Each group of tests was repeated three times, and the mean value was taken as the test result. The results are shown in Figure 3.

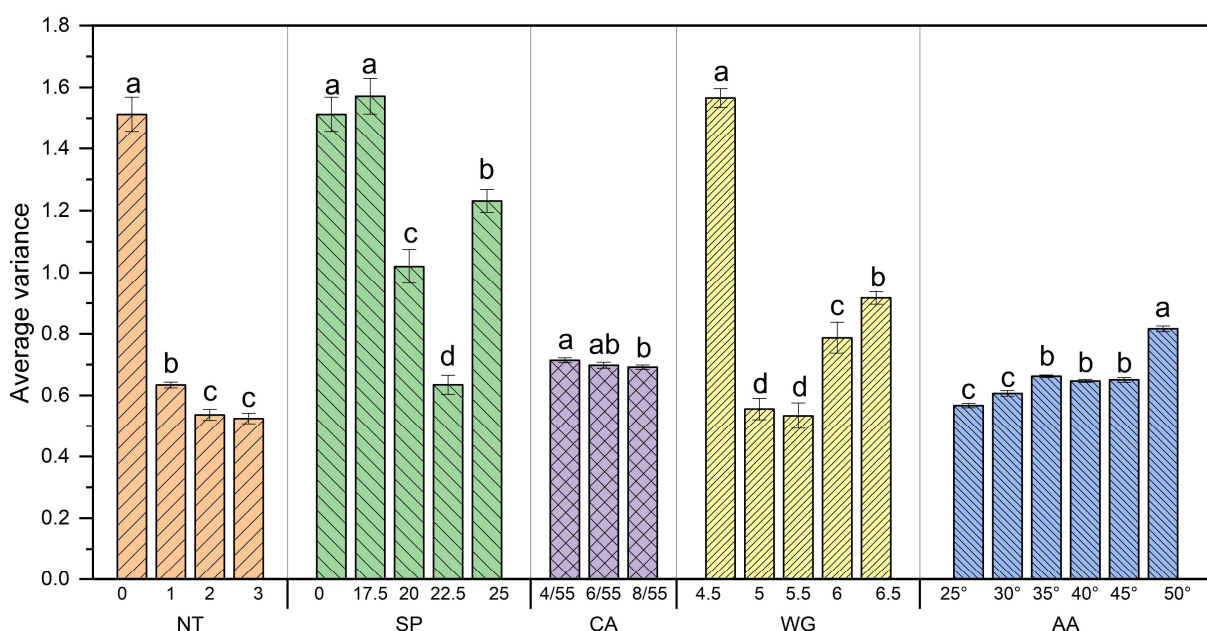


FIGURE 3. Single-factor test results.

Note: The same letter on the column indicates no significant difference between groups ($p>0.05$)

NT: number of threads; SP: screw pitch; CA: cone angle; WG: width of gap; AA: angle of air-tube

Effect of the number of threads on airflow uniformity

In this test, only the number of threads was changed, and other factors were fixed, SP=22.5 mm, CA=8/55, WG=5.5 mm, AA=35°. The number of threads NT was taken as 0, 1, 2 and 3.

The P value of the number of threads was less than 0.01 (Table 2), so this factor had a highly significant effect on the uniformity of the airflow field. As shown in Figure 3, the mean variance of airflow velocity in the test group was significantly lower than that in the control group, which indicated that the uniformity of the airflow field can be improved with an increasing number of threads. The addition of the number of threads improved the airflow path and changed the airflow from a disordered to an ordered state. In the test groups, there was no significant difference between the variance of the double-thread group and the three-thread group. Considering the difficulty of manufacturing, the double thread was set to the optimal level for this factor.

TABLE 2. Results of variance analysis of the number of threads.

Item	Sum of squares	Degree of freedom	Mean square	F value	P value
Among groups	0.017	2	0.009	20.914	0.002**
Within groups	0.002	6	0.000		
Sum	0.02	8			

Note: P ≤0.01, ** means extremely significant

Effect of screw pitch on the uniformity of airflow field

In this test, only the screw pitch was changed, and other factors were fixed, NT=2, CA=8/55, WG=5.5 mm, AA=35°. The screw pitch SP was taken as 17.5, 20, 22.5, 25 mm, and a control group without thread, respectively.

The P values for screw pitch were all less than 0.01 (Table 3), so this factor had a highly significant effect on the uniformity of the airflow field. As shown in Figure 3, compared to the control group, the mean variance of airflow velocity decreased in all test groups except the 17.5 mm test group. This shows that the addition of a suitable pitch can improve the uniformity of the airflow field. In the test group, with increasing screw pitch, the mean variance in airflow velocity decreased at first and then increased. When the screw pitch varied between 17.5 mm and 25 mm, as the screw pitch increased, the mean variance of the air velocity decreased sharply and then increased rapidly. The 22.5 mm test group had the lowest mean variance of airflow velocity, indicating that the flow field was most uniform at this point. Tests show that the uniformity of the airflow field was improved by increasing the screw pitch within a reasonable range. However, beyond a certain range, the uniformity of the airflow field worsened. It was possible that the airflow trajectory was not well corrected when the screw pitch was relatively large. Based on the analysis of the experimental results, the reasonable range of the screw pitch was 20-25 mm.

TABLE 3. Results of variance analysis of the screw pitch

Item	Sum of squares	Degree of freedom	Mean square	F value	P value
Among groups	0.905	3	0.302	77.926	0.000**
Within groups	0.031	8	0.004		
Sum	0.936	11			

Note: P ≤0.01, ** means extremely significant

Effect of cone angle on the uniformity of airflow field

In this test, only the cone angle was changed, and other factors were fixed, NT=2, SP=22.5 mm, WG=5.5 mm, AA=35°. The cone angle CA was taken as 4/55, 6/55 and 8/55.

The P value for screw pitch was 0.04 (Table 4), so this factor had a significant effect on the uniformity of the airflow field. As shown in Figure 3, when the cone angle varied between 4/55 and 8/55, with increasing cone angle, the mean variance of airflow velocity decreased gradually, indicating that the flow field became more uniform, but the change was small. The 8/55 test group had the lowest mean variance of airflow velocity, indicating that the flow field was most uniform at this point. Based on the analysis of the test results, a reasonable range of cone angles was 6/55-8/55.

TABLE 4. Results of variance analysis of the cone angle.

Item	Sum of squares	Degree of freedom	Mean square	F value	P value
Among groups	0.001	2	0.001	5.750	0.040*
Within groups	0.001	6	0.000		
Sum	0.002	8			

Note: 0.01 < P < 0.05, * means significant

Effect of width of gap on the uniformity of airflow field

In this test, only the width of the gap was changed, and other factors were fixed, NT=2, SP=22.5 mm, CA=8/55, AA=35°. The width of the gap WG was taken as 4.5, 5, 5.5 and 6 mm.

The P value for the width of the gap was less than 0.01 (Table 5), so the factor had a highly significant effect on the uniformity of the airflow field. As shown in Figure 3, with the increase in the width of the gap, the mean variance of airflow velocity decreased at first and then increased. The 5.5 mm test group had the lowest mean variance of airflow velocity, indicating that the flow field was most uniform at this point. The level of 5.5 mm was the optimal level for this factor. Based on the analysis of the test results, a reasonable range of the width of the gap was 5-6 mm.

TABLE 5. Results of variance analysis of the width of the gap.

Item	Sum of squares	Degree of freedom	Mean square	F value	P value
Among groups	0.585	4	0.146	337.763	0.000**
Within groups	0.004	10	0.000		
Sum	0.590	14			

Note: P ≤ 0.01 , ** means extremely significant

Effect of the angle of the air tube on the uniformity of the airflow field

In this test, only the angle of the air tube was changed, and other factors were fixed, NT=2, SP=22.5 mm, CA=8/55, and WG=5.5 mm. The angle of the air tube with the horizontal direction was taken as the test factor, and the angles of the air tube AA were taken as 25°, 30°, 35°, 40°, 45°, and 50°.

The P value of the angle of the air tube was less than 0.01 (Table 6), so this factor had a highly significant effect on the uniformity of the airflow field. As shown in Figure 3, when the angle of the air tube varied between 25° and 35°, as the angle of the air tube increased, the mean variance of the airflow velocity increased gradually, indicating that the flow field became turbulent. When the angle varied between 35°-45°, the mean variance of airflow velocity decreased as the angle of the inlet tube increased, but the change was small.

TABLE 7. Experimental design and variance mean results.

No.	X ₁ : Screw pitch/mm	X ₂ : Cone angle	X ₃ : Width of gap/mm	X ₄ : Angle of air tube/°	Mean variance of airflow velocity
1	-1	-1	-1	-1	0.83584
2	1	-1	-1	-1	0.46728
3	-1	1	-1	-1	0.79591
4	1	1	-1	-1	0.47423
5	-1	-1	1	-1	0.99200
6	1	-1	1	-1	0.68653
7	-1	1	1	-1	1.01719
8	1	1	1	-1	0.67212
9	-1	-1	-1	1	0.61066
10	1	-1	-1	1	0.80385
11	-1	1	-1	1	0.63668
12	1	1	-1	1	0.85082
13	-1	-1	1	1	0.73823
14	1	-1	1	1	0.98289
15	-1	1	1	1	0.80711
16	1	1	1	1	1.04579
17	-2	0	0	0	0.75299
18	2	0	0	0	0.64955
19	0	-2	0	0	0.61714
20	0	2	0	0	0.65679
21	0	0	-2	0	1.06648
22	0	0	2	0	1.42579
23	0	0	0	-2	0.57579
24	0	0	0	2	0.71498
25	0	0	0	0	0.62542
26	0	0	0	0	0.63542
27	0	0	0	0	0.60542
28	0	0	0	0	0.62916
29	0	0	0	0	0.62884
30	0	0	0	0	0.64164

When the angle varied between 45° and 50°, the mean variance of the airflow velocity showed a strongly increasing trend, indicating that the uniformity of the airflow field became turbulent as the angle of the air tube increased. The 25° test group had the lowest mean variance in airflow velocity, indicating that the flow field was most uniform at this point. The level of 25° was the optimal level for this factor. According to the analysis of the test results, the reasonable range of the angle of the air tube was 25°-45°.

TABLE 6. Results of variance analysis of the angle of the air tube.

Item	Sum of squares	Degree of freedom	Mean square	F value	P value
Among groups	0.160	5	0.032	54.928	0.000**
Within groups	0.007	12	0.001		
Sum	0.167	17			

Note: P ≤ 0.01 , ** means extremely significant

Results and analyses of the multifactor central composite test

To study the regularity of each factor on the uniformity of the airflow field, a multifactor central composite test was designed using Design-Expert 13.0. The results of the multifactor central composite test are shown in Table 7.

According to the experimental data in Table 7, the multiple regression fitting analysis was carried out by Design-Expert 13.0. After removing the insignificant regression terms, the regression model of the evaluation index is shown in [eq. (3)].

$$Y = 18.468 - 8.786 \times 10^{-2}X_1 + 2.786 \times 10^{-2}X_2 - 6.446X_3 - 1.383 \times 10^{-1}X_4 \\ + 5.532 \times 10^{-3}X_1X_4 + 2.469 \times 10^{-3}X_2X_4 + 2.317 \times 10^{-3}X_1^2 + 0.602X_3^2 \quad (3)$$

As shown in Figure 8, the P value of the regression model was less than 0.0001, indicating that the regression model was highly significant. The model misfit value was p=0.0886, and the P value was greater than 0.05, indicating that the model misfit value was not significant. In the fitted model, Factors X_1 , X_3 , X_4 , X_1X_4 , X_2X_4 , X_1^2 , and X_3^2 had a significant influence on this model. Other factors were not

significant. Based on the F value, the order of significance of the four influences was $X_3 > X_4 > X_1 > X_2$, and the model coefficient of determination R^2 was 0.9851, which indicated that the model could explain more than 98% of the variation in the response values and that this experimental regression model had a high level of reliability with a good degree of fit. Therefore, it could be used to analyse and predict test changes.

TABLE 8. Variance evaluation index quadratic polynomial model variance analysis.

Source	Sum of squares	Degree of freedom	Mean square	F value	P value
model	1.21	14	0.0865	212.50	< 0.0001
X_1	0.0190	1	0.0190	46.72	< 0.0001**
X_2	0.0014	1	0.0014	3.55	0.0791
X_3	0.2044	1	0.2044	502.19	< 0.0001**
X_4	0.0286	1	0.0286	70.33	< 0.0001**
X_1X_2	0.0000	1	0.0000	0.1106	0.7441
X_1X_3	0.0008	1	0.0008	1.90	0.1886
X_1X_4	0.3061	1	0.3061	752.13	< 0.0001**
X_2X_3	0.0005	1	0.0005	1.16	0.2977
X_2X_4	0.0024	1	0.0024	5.99	0.0271*
X_3X_4	0.0005	1	0.0005	1.33	0.2665
X_1^2	0.0052	1	0.0052	12.87	0.0027**
X_2^2	0.0007	1	0.0007	1.78	0.2017
X_3^2	0.6174	1	0.6174	1517.28	< 0.0001**
X_4^2	6.309E-07	1	6.309E-07	0.0016	0.9691
Residual	0.0061	15	0.0004		
Loss of fit term	0.0053	10	0.0005	3.52	0.0886
Pure error	0.0008	5	0.0002		
Sum	1.22	29			

Note: P ≤ 0.01, ** means extremely significant; 0.01 < P < 0.05, * means significant;

P > 0.05, means not significant.

Effects of test factors on evaluation index

The variance analysis of regression equations for the evaluation index is shown in Table 8. To analyse the relationship between the experimental factors and index more intuitively, the response surfaces were drawn in Design-Expert 13.0 (Figure 4).

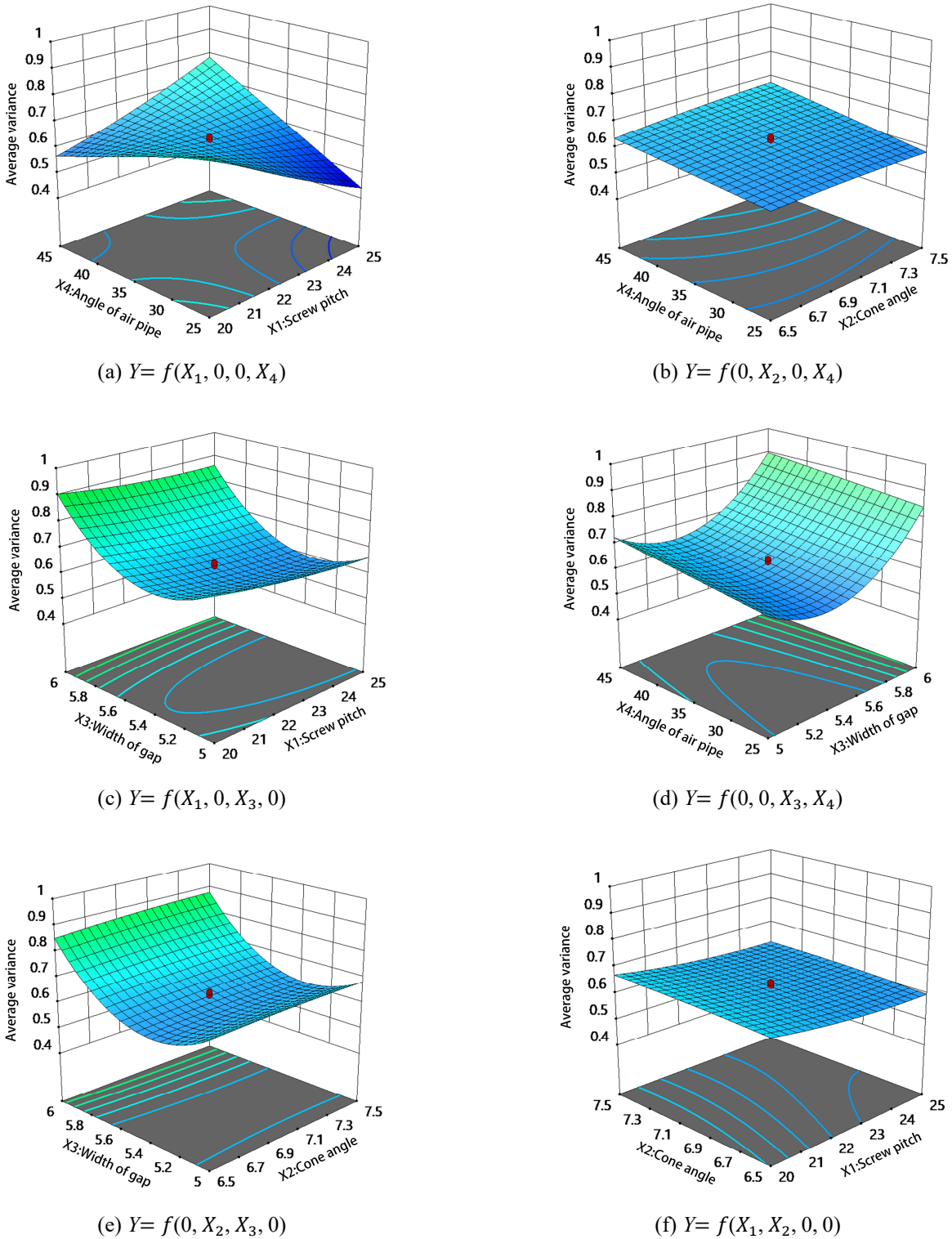


FIGURE 4. Effects of various factors on the index.

As shown in Figure 4a, the effects of screw pitch, angle of air-tube and their interaction on the mean variance of airflow velocity were all significant. When the screw pitch was smaller ($X_1 < 22$ mm), the mean variance of airflow velocity decreased with the increasing angle of the air tube. When the screw pitch was at a larger value ($X_1 > 22$ mm), the mean variance of airflow velocity increased with the increasing of the angle of the air-tube. The larger the screw pitch and the smaller the angle of the air tube, the smaller the mean variance of the airflow velocity. This was because with

increasing screw pitch, the thread became steeper, and the angle of the air tube relative to the thread decreased.

As shown in Figure 4b, the effect of cone angle on the mean variance of airflow velocity was insignificant, but the effect of both the angle of the air tube and the interaction of the two on the mean variance of airflow velocity were significant. The mean variance of airflow velocity increased slightly with increasing cone angle, but the change was small. The mean variance of the airflow velocity increased as the angle of the air tube increased. Reducing the angle of the air

tube allowed the airflow to make fuller use of the length of the threads. It could not only reduce the disordered collision of airflow but also improve the uniformity of the airflow field.

As shown in Figure 4c, the effects of screw pitch and gap width on the mean variance of airflow velocity were significant, but the interaction between the two was insignificant. The mean variance of airflow velocity decreased slightly with increasing screw pitch. When X_1 was approximately 25 mm, the test had the lowest mean variance of airflow velocity, indicating that the flow field was most uniform at this point. When the width of the gap was smaller ($X_3 < 5.3$ mm), the mean variance of airflow velocity decreased with increasing gap width. When the width of the gap was larger ($X_3 > 5.3$ mm), the mean variance of airflow velocity increased with increasing gap width.

As shown in Figure 4d, the effects of the width of the gap and the angle of the air tube on the mean variance of airflow velocity were significant, but the interaction between them was not significant. The mean variance of the airflow velocity increased with increasing air tube angle. When X_4 was approximately 25°, the test had the lowest mean variance of airflow velocity, indicating that the flow field is most uniform at this point. When the width of the gap was smaller ($X_3 < 5.2$ mm), the mean variance of airflow velocity decreased with increasing gap width. When the width of the gap was larger ($X_3 > 5.2$ mm), the mean variance of airflow velocity increased with increasing gap width. When X_3 was approximately 5.3 mm, the test had the lowest mean variance of airflow velocity, indicating that the flow field was most uniform at this point.

As shown in Figure 4e. The effect of the width of the gap on the mean variance of airflow velocity was significant, and the effect of cone angle and the interaction of the two on the mean variance of airflow velocity were insignificant. The mean variance of airflow velocity decreased slightly with increasing cone angle, but the change was small. When the width of the gap was smaller ($X_3 < 5.4$ mm), the mean variance of airflow velocity decreased with increasing gap width. When the width of the gap was larger ($X_3 > 5.4$ mm), the mean variance of airflow velocity increased with increasing gap width. When the width of the gap was between 5.2 and 5.4 mm, the test had the lowest mean variance of airflow velocity, indicating that the flow field was most uniform at this point.

As shown in Figure 4f, the effect of screw pitch on the mean variance of airflow velocity was significant, and the effect of cone angle and the interaction of the two on the mean variance of airflow velocity were insignificant. The mean variance of airflow velocity decreased slightly with increasing cone angle, but the change was small. The mean variance of airflow velocity decreased with increasing screw pitch. When the screw pitch was approximately 25 mm, the test had the lowest mean variance of airflow velocity, indicating that the flow field was most uniform at this point.

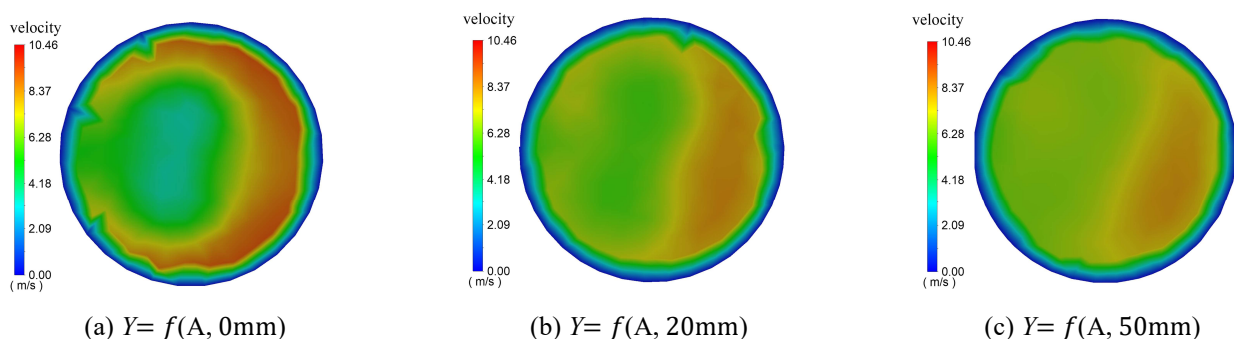
Validation tests

To obtain the optimal parameters, the optimization objectives of the lowest value of the mean variance of airflow velocity and boundary conditions of each factor provide the objective functions and constraints, and the constraint is shown in [eq. (4)].

$$\left\{ \begin{array}{l} \min Y(X_1, X_2, X_3, X_4) \\ 20 \text{ mm} < X_1 < 25 \text{ mm} \\ 6.5/55 < X_2 < 7.5/55 \\ 5 \text{ mm} < X_3 < 6 \text{ mm} \\ 25^\circ < X_4 < 45^\circ \end{array} \right. \quad (4)$$

According to the quadratic polynomial regression model established above, the optimization model of Design-Expert was used to solve the regression model. The results showed that the optimal parameters were $X_1=24.98$ mm, $X_2=7.47/55$, $X_3=5.31$ mm, and $X_4=25.09$. With these, the predicted value of the mean variance of the airflow velocity was $Y=0.412003$. To validate the accuracy of the model, the validation was carried out with the above optimized operating parameters, and there was a 4.65% deviation in the test results from the prediction value. The relative error value between the validation test and the predicted value was less than 5%. This showed that the experimental regression model had high reliability and indicated that the multifactor central composite test can effectively achieve optimization.

To visually show the comparison of preoptimization and post optimization results, velocity magnitude contours were plotted on the three selected planes, which were the plane at the seed-airflow intersection and the planes 20 and 50 mm away from it, as shown in Figure 5.



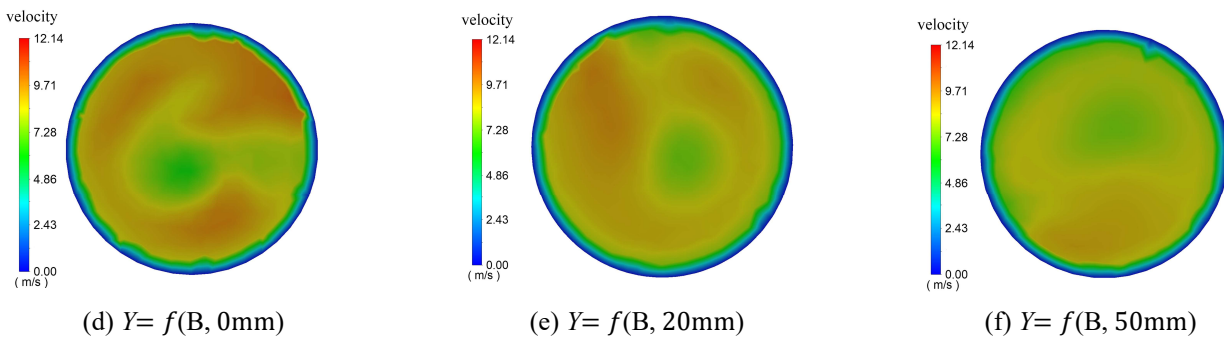


FIGURE 5. Velocity magnitude contours.

A: preoptimization B: after optimization

CONCLUSIONS

(1) To solve the serious problem of collisions between seeds and seed guide tubes in high-speed seeding, a high-speed seed guide device with conical spiral airflow was designed, which can use high-speed positive pressure airflow to transport seeds smoothly. The uniformity of the airflow field was mainly contributed by the thread structure set in the spiral accelerator.

(2) The single-factor test was carried out to investigate the effects of each factor on airflow uniformity and determine the reasonable range of values for each factor: number of threads $NT=2$, screw pitch $SP=20-25$ mm, cone angle $CA=6/55-8/55$, width of gap $WP=5-6$ mm, and angle of air tube $AA=25^\circ-45^\circ$.

(3) The four-factor and five-level central composite test was designed using the software Design-Expert 13.0. The results showed that the order of significance of the four factors was width of gap $X_3 >$ angle of air-tube $X_4 >$ screw pitch $X_1 >$ cone angle X_2 , and the optimal parameter combination was $X_1=24.98$ mm, $X_2=7.47/55$, $X_3=5.31$ mm, and $X_4=25.09^\circ$. The validation test showed that the relative error value between the validation test value and the predicted value was less than 5%. This shows that the quadratic fitting model can effectively predict the factor changes.

ACKNOWLEDGMENTS

This work was supported by the National Natural Science Foundation of China (Grant No. 52005307), Shandong Province Youth Innovation Team Development Plan of Universities (2022KJ225) and the National Key Research and Development Program of China (Grant No. 2021YFD2000401).

REFERENCES

- Carpes D, Alonço A, Rossato F, Veit A, Souza L, Francetto T (2017) Effect of different conductor tubes on the longitudinal distribution of corn seeds. *Revista Brasileira de Engenharia Agrícola e Ambiental* 21(9): 657-662.
<https://doi.org/10.1590/1807-1929/agriambi.v21n9p657-662>
- Chen X, Zhong L (2012) Design and test on belt-type seed delivery of air-suction metering device. *Transactions of the Chinese Society of Agricultural Engineering* 28(22): 8-15.
<https://doi.org/10.3969/j.issn.1002-6819.2012.22.002>
- Chen Y, Han J, Lan Y, Zhang M, Jin Y, Zhang Z, Wang W (2022) Design and experiment of the combined seed guiding tube for precision metering device. *Transactions of the Chinese Society of Agricultural Engineering* 38(24): 14-24.
<https://doi.org/10.11975/j.issn.1002-6819.2022.24.002>
- Dhillon G, Baarda L, Gretzinger M, Coles K (2022) Effect of precision planting and seeding rates on canola plant density and seed yield in southern Alberta. *Canadian Journal of Plant Science* 102(3): 698-709
- Ding Y, Yang L, Zhang D, Cui Tao, Li Y, Zhong X, Xie C, Ding Z (2021) Novel low-cost control system for large high-speed corn precision planters. *International Journal of Agricultural and Biological Engineering* 14(2): 151-158.
- Gao X, Xu Y, Yang L, Zhang D, Li Y, Cui T (2018) Simulation and experiment of uniformity of venturi feeding tube based on DEM-CFD coupling. *Transactions of the Chinese Society for Agricultural Machinery* 49(s1): 92-100.
<https://doi.org/10.6041/j.issn.1000-1298.2018.S0.013>
- Gao X, Zhao P, Li J, Xu Y, Huang Y, Wang L (2022) Design and experiment of quantitative seed feeding wheel of air-assisted high-speed precision seed metering device. *Agriculture-Basel* 12(11): 1951. <https://doi.org/10.3390/agriculture12111951>
- Kang J, Wen H, Wang S, Yan L (2015) Experimental study on impact of belt type conductor delivery on seeding uniformity. *Journal of Chinese Agricultural Mechanization* 36(05): 42-45.
<https://doi.org/10.13733/j.jcam.issn.2095-5553.2015.05.011>
- Kumar R, Raheman H (2018) Detection of flow of seeds in the seed delivery tube and choking of boot of a seed drill. *Computers and Electronics in Agriculture* 153: 266-277.
<https://doi.org/10.1016/j.compag.2018.08.035>
- Li Y, Yang L, Zhang D, Cui T, Zhang K, Xie C, Yang R (2020) Analysis and test of linear seeding process of maize high speed precision metering device with air suction. *Transactions of the Chinese Society of Agricultural Engineering* 36(09): 26-35.
<https://doi.org/10.11975/j.issn.1002-6819.2020.09.003>
- Liao Q, Shu C (2004) Study to determine the effect of precision planter tubes on uniformity of seeding. *Hubei Agricultural Sciences* 2004(04): 126-128+125.
<https://doi.org/10.14088/j.cnki.issn.0439-8114.2004.04.047>
- Liao Y, Li C, Liao Q, Wang L (2020) Research progress of seed guiding technology and device of planter. *Transactions of the Chinese Society for Agricultural Machinery* 51(12): 1-14.
<https://doi.org/10.6041/j.issn.1000-1298.2020.12.001>

- Liu J, Zhang P, Liu F (2016) The discrete element simulation guide tube height effects on seeding performance. *Journal of Agricultural Mechanization Research* 38(01): 12-16.
<https://doi.org/10.13427/j.cnki.njyi.2016.01.004>
- Liu R, Liu Y, Liu Z, Liu L (2023) Research on positive pressure airflow assisted blowing and seed guiding device of corn high-speed precision planter. *Transactions of the Chinese Society for Agricultural Machinery* 54(07): 156-166.
<https://doi.org/10.6041/j.issn.1000-1298.2023.07.015>
- Liu R, Liu Z, Zhao J, Lu Q, Liu L, Li Y (2022) Optimization and experiment of a disturbance-assisted seed filling high-speed vacuum seed-metering device based on DEM-CFD. *Agriculture-Basel* 12(9): 1304.
<https://doi.org/10.3390/agriculture12091304>
- Ma C, Yi S, Tao G, Li Y, Chen T, Liu H (2023) Mechanism analysis and parameter optimization of corn seeds receiving by rotating clamp of belt-type high-speed seed guiding device. *Transactions of the Chinese Society for Agricultural Machinery* 54(7): 134-143. <https://doi.org/10.6041/j.issn.1000-1298.2023.07.013>
- Nardon G, Botta G (2022) Prospective study of the technology for evaluating and measuring in-row seed spacing for precision planting: a review. *Spanish Journal of Agricultural Research* 20(4): e02R01. <https://doi.org/10.5424/sjar/2022204-19269>
- Wang C, Li H, He J, Wang Q, Lu C, Wang J (2020 a) Design and experiment of pneumatic wheat precision seed casting device in rice-wheat rotation areas. *Transactions of the Chinese Society for Agricultural Machinery* 2020,51(05): 43-53.
<https://doi.org/10.6041/j.issn.1000-1298.2020.05.005>
- Wang G, Shi R, Mi L, Hu J (2022 a) Agricultural eco-efficiency: challenges and progress. *Sustainability* 14(3): 1051.
<https://doi.org/10.3390/su14031051>
- Wang J, Tang H, Wang J, Shen H, Feng X, Huang H (2017) Analysis and experiment of guiding and dropping migratory mechanism on pickup finger precision seed metering device for corn. *Transactions of the Chinese Society for Agricultural Machinery* 48(1): 29-37. <https://doi.org/10.6041/j.issn.1000-1298.2017.01.005>
- Wang W, Zhang S, Li J, Zhang P, Chen Y (2022 b) Effects of the win-row planter with subsoiling on soybean growth and yield in northern China. *Journal of Agricultural Engineering* 53(3): 1359. <https://doi.org/10.4081/jae.2022.1359>
- Wang Y, Zhang W, Yan W, Qi B (2020 b) Design and experiment of seed pressing device for precision seeder based on air flow assisted seed delivery. *Transactions of the Chinese Society for Agricultural Machinery* 51(10): 69-76.
<https://doi.org/10.6041/j.issn.1000-1298.2020.10.009>
- Wei M, Diao P, Wang W (2022) Design and experiment of the seed delivery device with a rotating brush wheel for precision seeder. *Engenharia Agrícola* 42(6): e20220089.
<https://doi.org/10.1590/1809-4430-Eng.Agric.v42n6e20220089/2022>
- Yang L, Yan B, Zhang D, Zhang T, Wang Y, Cui T (2016) Research progress on precision planting technology of maize. *Transactions of the Chinese Society for Agricultural Machinery* 47(11): 38-48. <https://doi.org/10.6041/j.issn.1000-1298.2016.11.006>
- Yang W, Zhang X, Zhong G, Zheng J, Pu W, Ma Y (2022) Design and experiment of seed tube of seedling planter for panax notoginseng. *Journal of South China Agricultural University* 43(1): 120-132. <https://doi.org/10.7671/j.issn.1001-411X.202104007>
- Yuan Y, Bai H, Fang X, Wang D, Zhou L, Niu K (2018) Research progress on maize seeding and its measurement and control technology. *Transactions of the Chinese Society for Agricultural Machinery* 49(9): 1-18.
<https://doi.org/10.6041/j.issn.1000-1298.2018.09.001>
- Zhao S, Chen J, Wang J, Chen J, Yang C, Yang Y (2018) Design and experiment on V-groove dialing round type guiding-seed device. *Transactions of the Chinese Society for Agricultural Machinery* 49(6): 146-158. <https://doi.org/10.6041/j.issn.1000-1298.2018.06.017>
- Zhou L, Yu J, Wang Y, Yan D, Yu Y (2020) A study on the modelling method of maize-seed particles based on the discrete element method. *Powder Technology* 374: 353-376.
<https://doi.org/10.1016/j.powtec.2020.07.051>